

# Practical Advantages of the Local Strain Energy Approach for Fatigue Strength Assessments of Welded Joints

F. Berto<sup>1</sup>, P. Lazzarin<sup>1</sup>, M. Zappalorto<sup>1</sup>, F.J. Gómez<sup>2</sup>  
<sup>1</sup> *University of Padova, Vicenza, Italy;*  
<sup>2</sup> *Universidad Politécnica de Madrid, Spain.*

**Abstract.** Dealing with the notch stress intensity approach applied to the fatigue assessment of welded joints, the weld toe is modelled as a sharp V-notch. While the Notch Stress Intensity Factors (NSIFs) evaluation requires a very accurate mesh in the vicinity of the point of singularity, which is the weakness of the approach in the presence of complex structures, the mean value of the elastic Strain Energy Density (SED) on the control volume can be determined with high precision by using a coarse mesh. This property of SED is analysed in the present paper by using a number of FE models with very different mesh refinements. Both bi-dimensional and three-dimensional welded details have been considered.

## 1. Introduction

The current approaches for the fatigue strength assessment of welded joints can mainly be divided into categories depending on the type of the stress analysis performed [1]. One can distinguish criteria based on nominal stress, structural stress, local stress or local strain as well as other approaches based on linear elastic Fracture Mechanics [2,3]. These approaches are separately summarised in the most recent Recommendations [4].

The main problems occurring in the application of local criteria are tied to the degree of arbitrariness in precisely defining the geometrical parameters [5]. The Effective Notch Stress method [6,7], suggests the introduction of a fictitious notch radius at the critical point of the structure. On the contrary, in the notch stress intensity approach [8-10], the concept of notch rounding is not applied and the weld toe is modelled as a sharp V-notch. Thus, the mode I and mode II Notch Stress Intensity Factors (NSIFs) can be used to quantify the magnitude of the asymptotic stress distribution [11]. In principle NSIFs are used to describe crack initiation at sharp notches [12, 13] just as stress intensity factors (SIFs) at crack-like notches. Afterwards it was shown that the use of  $S-N$  curve in terms of NSIFs is possible in the medium life regime. In fact a large amount of the fatigue life is spent with a short crack fully embedded in a zone governed by the V-notch singularity. For its application the NSIF approach requires the knowledge of the elastic stress field in the region very close to the point of singularity. With this aim FE meshes must be very refined in the neighbourhood of the notch tip. The refinement required is far from easy to obtain in plane cases and very difficult and time expensive in three-dimensional cases. Some different approaches have been proposed to overcome the difficulties tied to mesh refinements [14-19]. Among the others, the structural stress method releases the requirements of small mesh size [16]. In Dong's model [17] the intensity of the structural stress distribution at the weld toe is obtained by considering a combination of bending and membrane stress on a surface normal to the applied load and located at the distance from the

weld toe equal to the main plate thickness. Dong's method and other calculation methods for structural stress at welded joints have been revisited by Doerk *et al.* [18] and by Poutianen and Marquis [19]. The conventional structural stress method was modified [16] by considering the stress in the weld for partial and full-load carrying fillet weld. It was highlighted that welds of different types (butt or fillet) or with different geometries may have different fatigue strengths even though the structural stress is the same. To overcome this problem, a method based on a multi-linear stress distribution that depends on the stress in the weld, the weld size and the plate thickness was proposed in Ref. [16]. The semi-empirical thickness correction, such as that used in the conventional structural stress method is no longer necessary. Good agreement was found between fatigue assessment based on the new criterion, LEFM-based results and many experimental data. The main advantage is that a relatively coarse mesh is required for the application of the method.

Dealing with local approaches and coarse meshes an extension of the Nisitani and Teranishi's method [15], successfully formalised for cracked components, has been recently proposed for welded structures by Meneghetti and Lazzarin [14]. After a calibration process, it was possible to give a closed-form expression able to estimate the NSIF from a fictitious peak stress on the point of singularity by means of a coarse mesh pattern with a constant element size.

Following the local approach philosophy and not the method based on a structural stress, the present paper deals with the use of the mean value of the elastic Strain Energy Density (SED) on a control volume for the assessment of fatigue strength of welded structures. The main hypotheses remain those at the basis of the NSIF approach and the weld toe is modelled as a sharp V-notch. Varying the toe angle the direct comparability of the NSIFs is no longer possible and the stress intensity factor of the slit end at the weld root has a different unit of measure from that of the NSIF at the weld toe. A direct comparison can be performed by using the SED averaged over a control volume surrounding the weld root or weld toe as fatigue relevant parameter. In some previous papers [20-22], this parameter was expressed in closed form on the basis of the relevant NSIFs, and the radius  $R_0$  of the averaging zone was found to be 0.28 mm and 0.12 mm for welded joints made of steel and aluminium alloy respectively [20- 22]. The main aim of the present paper is to demonstrate that, as opposed to the direct evaluation of the NSIFs, the mean value of the elastic SED on the control volume can be accurately determined by using relatively coarse meshes. This fact is of major importance for the application of the method to components of complex geometry [23].

## **2. The link between SED and NSIF**

The degree of the singularity of the stress fields due to re-entrant corners was established by Williams [11] both for mode I and mode II loading (see also Ref. [1]). When the weld toe radius  $\rho$  is set to zero, NSIFs quantify the intensity of the asymptotic stress distributions in the close neighbourhood of the notch tip. By using a polar coordinate system  $(r, \theta)$  having its origin located at the sharp notch tip, the NSIFs related to mode I and mode II stress distributions are [24]:

$$K_1 = \sqrt{2\pi} \lim_{r \rightarrow 0^+} r^{1-\lambda_1} \sigma_{\theta\theta}(r, \theta = 0) \quad K_2 = \sqrt{2\pi} \lim_{r \rightarrow 0^+} r^{1-\lambda_2} \sigma_{r\theta}(r, \theta = 0) \quad (1)$$

Under plane strain conditions, the total elastic strain energy density averaged over a sector of radius  $R_0$  is

$$\Delta \bar{W} = \frac{e_1}{E} \left[ \frac{\Delta K_1}{R_0^{1-\lambda_1}} \right]^2 + \frac{e_2}{E} \left[ \frac{\Delta K_2}{R_0^{1-\lambda_2}} \right]^2 \quad (2)$$

where the parameters  $e_1$  and  $e_2$  depend on the notch opening angle  $2\alpha$  and the Poisson's ratio  $\nu$  [20]. When the V-notch angle  $2\alpha$  is 135 degrees, a typical value for fillet welded joints, the mode I stress distribution is singular ( $1-\lambda_1=0.326$ ) whereas the mode II distribution is not ( $1-\lambda_2= -0.302$ ). Consequently eq.(2) can be simplified in the form:

$$\Delta \bar{W} = \frac{e_1}{E} \left[ \frac{\Delta K_1}{R_0^{1-\lambda_1}} \right]^2 \quad (3)$$

where the circular sector with radius  $R_0$  should be fully included in the zone governed by the mode I singularity. Parameter  $e_1$  is 0.1172 for  $2\alpha=135^\circ$  and a Poisson's ratio  $\nu=0.3$  [20]. When the von Mises criterion is applied instead of the Beltrami criterion, the value for  $e_1$  changes and becomes independent of  $\nu$  [20]. An application of the mean value of the deviatoric strain energy density over a control volume was reported in Ref. [25], where the fatigue behaviour of welded components under multi-axial loading was analysed.

Dealing with the strain energy density, it is necessary to mention Sih's criterion based on the strain energy density factor S [26]. The parameter S is the product of the strain energy density and a small distance from the point of singularity. Failure is thought of as controlled by a critical value of S, whereas the direction of crack propagation is determined by imposing a minimum condition on S. However, as highlighted by Yosibash *et al.* [27], who also proposed the SED approach to assess the static strength of V-notched components made of brittle materials, Sih's criterion is a point-related criterion: the minimum of S, correlated to a material-dependent parameter, is the failure criterion. Conversely, the area- or volume-related averaged value of the SED does not predict the direction of crack propagation, but predicts only failure initiation at a specific critical value, which is independent of the V-notch angle.

The  $\Delta W-N$  scatterband already proposed by Lazzarin *et al.* [21] on the basis of about 280 fatigue data was applied to 650 fatigue data mainly from fillet cruciform welded joints (non-load carrying and load-carrying) with final fractures originating from the weld toe or the weld root [22]. In all those cases, the weld toe (or the weld root) was modelled like a sharp notch,  $\rho = 0$  (V-notch or crack). The scatter index  $T_W$ , related to probabilities of survival  $P_S=2.3\%$  and  $97.7\%$ , is 3.3. However, it becomes 1.50 if converted into an equivalent local stress range with probabilities of survival  $P_S=10\%$  and  $90\%$ , in agreement with Haibach's normalised  $S-N$  curve [28]. Recently, the scatterband has been successfully applied to butt welded joints made of structural steels [29]. The control radius shown was evaluated by using the following expression [20-22]:

$$R_0 = \left( \sqrt{2e_1} \times \frac{\Delta K_{IA}}{\Delta \sigma_A} \right)^{\frac{1}{1-\lambda_1}} = \left( \sqrt{2 \times 0.117} \times \frac{211}{155} \right)^{\frac{1}{1-0.674}} = 0.28 \text{ mm} \quad (4)$$

where the values of the parameters  $\Delta K_{IA}$  and  $\Delta \sigma_A$  (both referred to  $N_A=5 \times 10^6$  cycles to failure and to a probability of survival  $P_s=50\%$ ) were determined by using data taken from the literature. In particular,  $\Delta K_{IA} = 211 \text{ MPa}(\text{mm})^{0.326}$  is the mode I NSIF range as initially determined from fillet welded joints with a V-notch opening angle equal to  $135^\circ$  at the weld toe [10] whereas  $\Delta \sigma_A$  is the stress range from butt-welded joints ground flush to plate [30].

### 3. The use of a coarse mesh to evaluate SED in 2D and 3D welded joints

#### 3.1 Bi-dimensional models

In order to demonstrate some interesting features of the local SED-based approach, a number of different geometries related to transverse non-load-carrying fillet welded joints have been considered (Figure 1). The geometrical parameters listed in Table 1 match those characterizing the welded joints analyzed in the past by Maddox [2] and Gurney [3], who determined experimentally the fatigue strength properties and compared experimental data and theoretical predictions carried out on the basis of Linear Elastic Fracture Mechanics. The same set of experimental data was used by other researchers to check the NSIF approach [8, 10] and a modified structural stress approach, as recently formulated by Poutianen and Marquis [16].

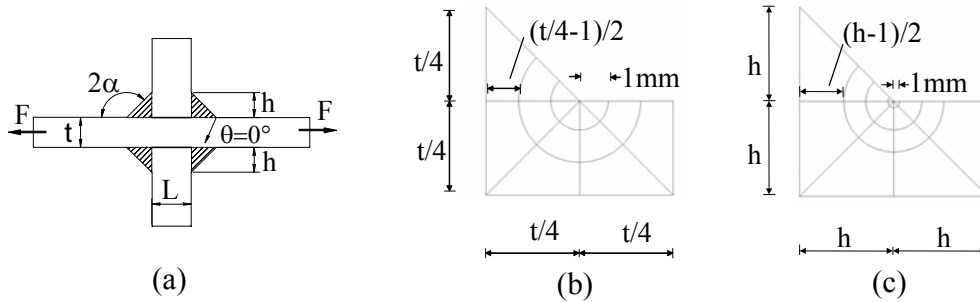


Figure 1: Geometrical parameters for transverse non-load carrying fillet welded joints Modulus used for the geometries with  $h > t/2$  (b); modulus used when  $h < t/2$  (c)

While taking advantage of the double symmetry, only a quarter of the geometry could be modelled. In particular, the highly stressed region ahead of the weld toe has been modelled by means of the mesh patterns shown in Figure 1. In a limited number of cases (series 1, 5 and 8) the height  $h$  of the bead was greater than  $t/2$ . For these three series the modulus shown in Figure 1b was used. An additional row of finite elements completes the geometry up to the longitudinal axis of symmetry. One should note that the row 1 (the line closer to the V-notch tip) decides the mesh pattern whereas the row 2 adapts itself as a function of the row 1. The modulus includes 15 linear or quadratic finite elements. In particular, considering plane strain conditions, Plane 82 or Plane 42, as implemented in the ANSYS<sup>®</sup> code, were used. With the aim to reduce the number of degrees of

freedom in the FE models a control radius  $R^* = 1.0$  mm is assumed. It is possible to revert the local strain energy density (as directly obtained from the FE model) to the ‘actual’ control volume by using the expression:

$$\overline{W}(R_0 = 0.28) = \frac{\overline{W}(R^* = 1.0)}{[R_0 / R^*]^{2(1-\lambda)}} = \beta \times \overline{W}(R^* = 1.0) \quad (5)$$

where  $\beta=2.293$  for  $2\alpha=135$  degrees. The radius  $R^*$  in eq. (5) should not exceed the size of the zone governed by the mode I singularity. Precise information about this topic was given in Ref. [8] as a function of the main plate thickness  $t$  and the weld height  $h$ . When  $2\alpha=0$  one should introduce  $\beta=3.571$  in eq. (5). In the other 9 series, the condition  $h < t/2$  was assured and  $h$  becomes the parameter that controls the modulus size (Figure 1c). Like in the previous models, another row of finite elements is typically used to complete the geometry.

Series	t [mm]	h [mm]	L [mm]	Fine mesh	Parabolic FE (Coarse mesh)		
				$K_I$ [MPa mm <sup>0.326</sup> ]	$\overline{W}$ [N mm/mm <sup>3</sup> ]	$K_I$ [MPa mm <sup>0.326</sup> ]	$\Delta$ %
1	13	8	10	265.0	$4.28 \times 10^{-2}$	274.3	3.5
2	50	16	50	396.	$9.07 \times 10^{-2}$	399.3	0.7
3	100	16	50	413.0	$9.94 \times 10^{-2}$	417.9	1.2
4	13	5	3	228.8	$3.25 \times 10^{-2}$	238.9	4.4
5	13	10	8	267.5	$4.23 \times 10^{-2}$	272.8	2.0
6	25	5	3	231.0	$3.32 \times 10^{-2}$	241.6	4.6
7	25	9	32	329.5	$6.11 \times 10^{-2}$	327.7	-0.5
8	25	15	220	405.0	$9.08 \times 10^{-2}$	399.4	-1.4
9	38	8	13	296.7	$5.21 \times 10^{-2}$	302.5	2.0
10	38	15	220	476.0	$1.25 \times 10^{-1}$	469.0	-1.5
11	100	5	3	228.1	$3.28 \times 10^{-2}$	240.2	5.3
12	100	15	220	589.5	$1.87 \times 10^{-1}$	573.0	-2.8

Table 1. Comparison between the values of the NSIFs evaluated with very fine meshes and coarse meshes taking advantage of eq. (6) linking the local SED and the mode I NSIF. Geometries according to Maddox [2] and Gurney [3], see Fig.1. The remotely applied nominal stress is equal to 100 MPa.

Two rows were necessary only for two models with  $h < t/6$  (model 3, where  $h=16$  mm and  $t=100$  mm, and model 11 where  $h=5$  mm and  $t=100$  mm). As far as the transverse plate is concerned, only a column of finite elements was usually used when  $L$  was equal to or less than 50 mm. Two or three columns of FE was used only when  $L=220$  mm, depending on the main plate thickness. The total number of FE ranges from 35 to 56. Differently from the NSIF evaluation, which needs a very fine mesh in the vicinity of the point of singularity it will be shown that the mean value of the local SED is substantially independent of the mesh size. It has

to be noted that the SED is available in the postprocessor of ANSYS and other codes as an easy-to-call function.

In the present paper, for direct comparison with coarse models, all the geometries have also been analysed by using very fine meshes, as it is usually done when the main aim of the research is the direct evaluation of the NSIFs. Once the SED values from the coarse models have been determined, due to the non-singularity of the mode II stress components, the mode I NSIF can be derived by using the following relationship:

$$K_I = (R^*)^{1-\lambda_1} \sqrt{\frac{E \bar{W}}{e_1}} = 2.921 \sqrt{E \bar{W}} \quad (6)$$

where, for a V-notch opening angle  $2\alpha=135$  degrees,  $1-\lambda_1=0.326$  and  $e_1=0.1172$  (see Refs.[20-22]). Obviously, the coefficient 2.921 reported on the right hand side of eq.(6) is valid only for  $R^*=1.0$  mm, *i.e* for the control radius suggested herein. However, the coefficient can be easily updated for different values of  $2\alpha$  and  $R^*$ . The values of the NSIFs obtained by means of eq. (6) for all the joints are reported in table 1 and are compared to those obtained by means of very fine meshes. By using quadratic elements the maximum error between the  $K_I$  values as determined by means of very fine meshes and those from coarse meshes is 5.3 percent (see Table 1, series 11). The error decreases to about 4.5 percent for the series 4 and 6. Note that these three series present a very small value of the transverse plate thickness,  $L=3$  mm. In all the other geometries the error is really very small, being usually less than 3 percent.

### 3.2 Three-dimensional models

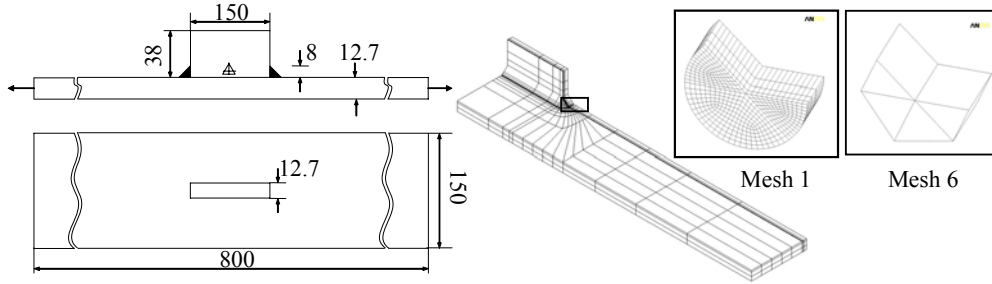


Figure 2: Welded joint with a longitudinal stiffener (one quarter of the geometry); detail of the control volume with  $R^*=1$  mm.

The longitudinal non-load-carrying welded joints represented schematically in Figure 2 have been analysed herein in terms of SED over a control volume. The same geometry was analysed by Maddox in Ref. [31]. A typical FE model is shown in the Figure 2. Very different meshes have been drawn in the FE simulations, as documented in Figure 2 with reference only to the control volume where the most fine mesh, named ‘*mesh 1*’ and the coarsest mesh, called ‘*mesh 6*’, are shown. In principle, stress gradients can be present not only in the radial direction (according to William’s plane solution) but also in the direction parallel

to the line drawn by the V-notch tips (*i.e.* the weld direction). Then, to account for these secondary stress gradients, the SED should be determined in a volume having a depth approximately equal to  $R^*$ . Precise information about the number of FE used to model the control volume and the degrees of freedom characterising the entire models are summarised in Table 2. All analyses have been carried out by using 20 node solid finite elements (named Solid95 in the ANSYS<sup>®</sup> code).

3D models	Number of FE in the volume	Degrees of freedom (complete model)	$\overline{W}$ [Nmm/mm <sup>3</sup> ]	$K_1$ [MPa mm <sup>0.326</sup> ]	$\Delta\%$
1	1696	$8.6 \cdot 10^5$	0.07937	373.5	0
2	768	$4.6 \cdot 10^5$	0.07903	372.7	0.21
3	324	$2.5 \cdot 10^5$	0.07896	372.5	0.26
4	96	$1.7 \cdot 10^5$	0.07895	372.5	0.26
5	24	$4.5 \cdot 10^4$	0.07790	370.0	0.93
6	4	$1.1 \cdot 10^4$	0.07594	365.3	2.18

Table 2. Results from the 3D models of the welded joint with a longitudinal stiffener shown in Fig. 2 (remotely applied nominal stress equal to 100 MPa,  $R^* = 1$  mm)

The results of the linear elastic analyses are listed in terms of the mean value of SED in Table 2. Here the results are all related to a nominal stress,  $\sigma_{nom}$ , equal to 100 MPa. It is evident that the maximum difference between the models with very refined meshes and coarse meshes is 5 percent. Taking advantage of the value of the local SED, the NSIF related to the welded detail can be determined *a posteriori* by simply using eq. (6), considering tacitly verified the plane strain hypothesis.

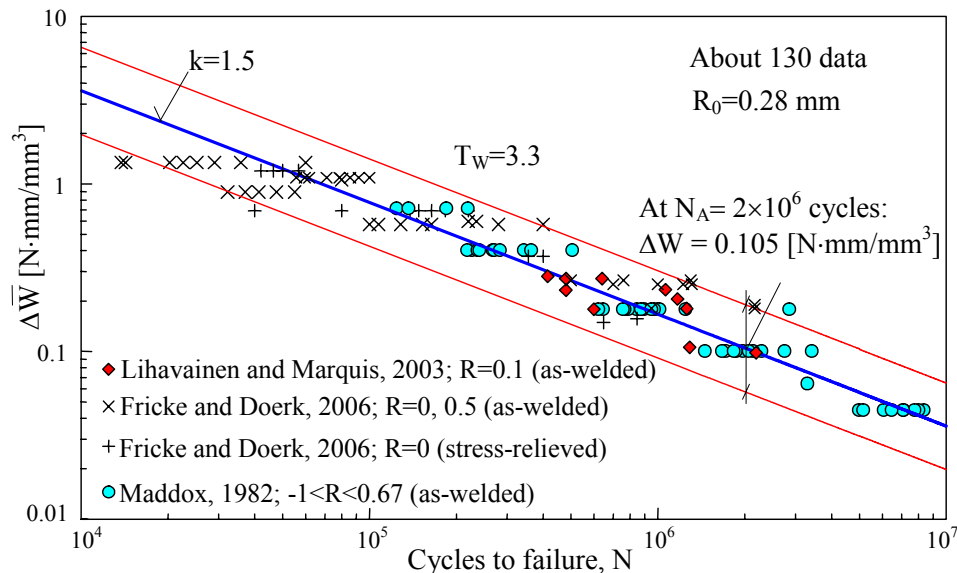


Figure 3. Fatigue strength of the welded joints made of structural steel in terms of local strain energy density; comparison with the scatter band proposed in Refs [21, 22]

#### 4. Fatigue strength of complex steel welded joint made in terms of SED

The main geometric parameters of the welded joints considered here as well as the loading conditions are summarised in Ref. [23]. Original data are reported in Refs [31-33]. The strain energy has been evaluated by means of three-dimensional finite element analyses carried out with Ansys 9.0<sup>®</sup> and using as control volume a circular sector with  $R_0=0.28$  mm.

In Figure 3 experimental data reconverted in terms of the mean values of the local SED are successfully compared with the theoretical scatter band reported in Refs [21, 22]. The scatter index  $T_W$ , related to probabilities of survival  $P_S=2.3\%$  and  $97.7\%$ , is found to be 3.3.

#### 5. Final remarks and future developments

The powerful property of SED and the practical application of coarse meshes discussed in the present paper were applied also to elastic-plastic V-notched plates under tension loading and V-notched round bar under torsion [34] showing that also when the material behaviour obeys a power hardening law, the SED over a control volume can be precisely determined from a rough mesh. A sound theoretical justification of the mesh refinement independency will be proposed in a forthcoming publication where other basic, but not ‘trivial’, samples will be presented.

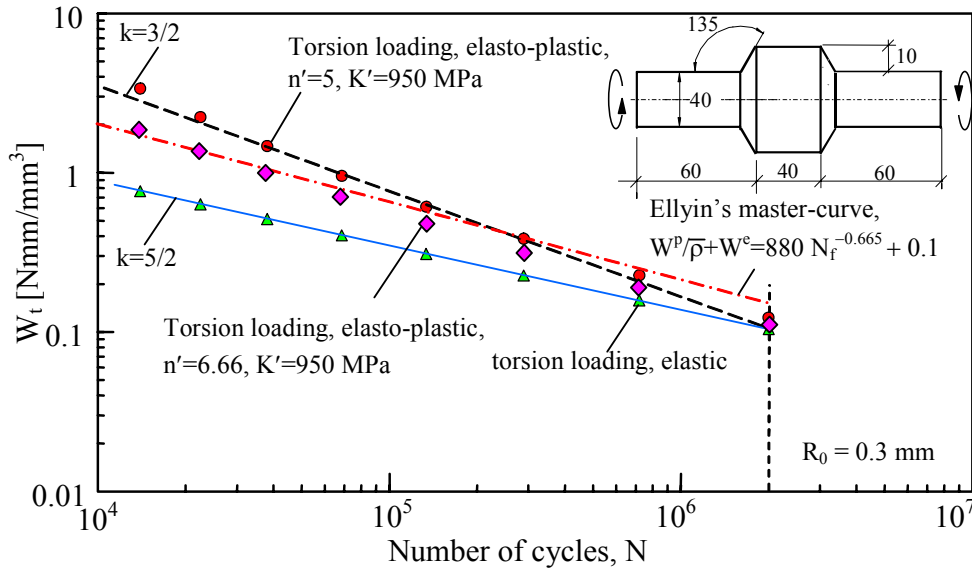


Figure 4. Total SED under linear elastic and elastic-plastic conditions

The different role played by local and large scale yielding under tension and torsion loading provided an interesting interpretation for the different slopes, 3.0 and 5.0, reported by Eurocode 3 and other Standards in force for welded details subjected to tensile or shear stresses, respectively [34]. A very satisfactory agreement was found between the scatterband obtained by considering as main failure parameter the averaged SED and Ellyin's *fatigue master life curve* based on the use of the plastic strain energy per cycle  $\Delta \tilde{W}^P$  as evaluated from the closed

cyclic *hysteresis loop* and the positive part of the elastic strain energy density  $\Delta\tilde{W}^{e+}$  [35].

## References

- [1 ] Radaj D, Sonsino CM, Fricke W. *Fatigue assessment of welded joints by local approaches*, Woodhead Publishing, Cambridge, 2006, 2nd edn.
- [2 ] Maddox. S.J. (1987). *The Effect of Plate Thickness on the Fatigue Strength of Fillet Welded Joints*. Abington Publishing, Abington, Cambridge.
- [3 ] Gurney, TR. (1991). *The fatigue strength of transverse fillet welded joints*. Abington Publishing, Cambridge.
- [4 ] Hobbacher A (Ed.). *Fatigue design of welded joints and components*, Abington Publishing, Cambridge 2005 (updated edn.).
- [5 ] Radaj D. Review of fatigue strength assessment of nonwelded and welded structures based on local parameters. *Int J Fatigue* 1996;18 (3):153-170.
- [6 ] Radaj D. Näherungsweise Berechnung der Formzahl von Schweißnähten. *Schw. Schn.* 1969;21(3): 97-105, and 21(4):151-158.
- [7 ] Radaj, D. *Design and analysis of fatigue resistant welded structures*, Abington Publishing, Cambridge 1990.
- [8 ] Lazzarin P, Tovo R. A Notch Intensity Approach to the Stress Analysis of Welds. *Fatigue Fract Eng Mater Struct* 1998;21:1089-1104.
- [9 ] Tovo R, Lazzarin P. Relationships between local and structural stress in the evaluation of the weld toe stress distribution, *Int J Fatigue* 1999;21:1063-1078.
- [10 ] Lazzarin P, Livieri P. Notch Stress Intensity Factors and fatigue strength of aluminium and steel welded joints. *Int J Fatigue* 2001;23:225-232.
- [11 ] Williams ML. Stress singularities resulting from various boundary conditions in angular corners on plates in tension. *J Applied Mech* 1952;19:526-528.
- [12 ] Boukharouba T, Tamine T, Nui L, Chehimi C, Pluvinage G.. The use of notch stress intensity factor as a fatigue crack initiation parameter. *Engng Fract Mech* 1995;52:503-512.
- [13 ] Verreman Y, Nie B. Early development of fatigue cracking at manual fillet welds. *Fatigue Fract Eng Mater Struct* 1996;19:669-681.
- [14 ] Meneghetti G, Lazzarin P. Significance of the Elastic Peak Stress evaluated by FE analyses at the point of singularity of sharp V-notched components. *Fatigue Fract Engng Mater Struct* 2007;30:95-106.
- [15 ] Nisitani H, Teranishi T.  $K_I$  value of a circumferential crack emanating from an ellipsoidal cavity obtained by the crack tip stress method in FEM. *Engng Fract Mech* 2004;71:579-585.
- [16 ] Poutiainen I, Marquis G. A fatigue assessment method based on welded stress. *Int J Fatigue* 2006;28:1037-1046.
- [17 ] Dong P. A structural stress definition and numerical implementation for fatigue analysis of welded joints. *Int J Fatigue* 2001; 23:865-876.
- [18 ] Doerk O, Fricke W, Weissenborn C. Comparison of different calculation methods for structural stresses at welded joints. *Int J Fatigue* 2003;25, 359-369.

- [19 ] Poutiainen I, Tanskanen P, Marquis G. Finite element methods for structural hot spot stress determination – a comparison of procedures. *Int J Fatigue* 2004;26:1147-1157.
- [20 ] Lazzarin P, Zambardi R. A finite-volume-energy based approach to predict the static and fatigue behaviour of components with sharp V-shaped notches. *Int J Fract* 2001;112:275-298.
- [21 ] Lazzarin P, Lassen T, Livieri P. A Notch Stress Intensity approach applied to fatigue life predictions of welded joints with different local toe geometry. *Fatigue Fract Engng Mater Struct* 2003;26:49-58.
- [22 ] Livieri P, Lazzarin P. Fatigue strength of steel and aluminium welded joints based on generalised stress intensity factors and local strain energy values. *Int J Fract* 2005;133:247-276.
- [23 ] Lazzarin P., Berto F., Gomez FJ., Zappalorto M. (2008) Some advantages derived from the use of the strain energy density over a control volume in fatigue strength assessments of welded joints. *International Journal of Fatigue*, 30, 1345-1357.
- [24 ] Gross R, Mendelson A. Plane Elastostatic Analysis of V-Notched Plates. *Int J Fract Mech* 1972;8:267-72.
- [25 ] Lazzarin P, Sonsino CM, Zambardi R. A Notch Stress Intensity approach to predict the fatigue behaviour of T butt welds between tube and flange when subjected to in-phase bending and torsion loading. *Fatigue Fract Engng Mater Struct* 2004;27:127-141.
- [26 ] Sih GC. Strain-energy-density factor applied to mixed mode crack problems. *Int J Fract* 1974;10:305-321.
- [27 ] Yosibash Z, Bussiba Ar, Gilad I. Failure criteria for brittle elastic materials. *Int J Fract* 2004;125:307-333
- [28 ] Haibach E. *Service fatigue strength – methods and data for structural analysis* (in German), Springer Verlag, Berlin 2002.
- [29 ] Lazzarin P, Berto F, Radaj D. Uniform fatigue strength of butt and fillet welded joints in terms of the local strain energy density. Proc. IFC9, 2006, Atlanta, USA. On CD Rom.
- [30 ] Atzori B, Dattoma V A comparison of the fatigue behaviour of welded joints in steels and in aluminium alloys. IIW 1983; Document XXXIII-1089-1983.
- [31 ] Maddox SJ. Influence of tensile residual stresses on the fatigue behavior of welded joints in steel. ASTM STP. 1982; 776: 63-96.
- [32 ] Lihavainen VM, Marquis G. Fatigue strength of a longitudinal attachment improved by ultrasonic impact treatment. IIW. 2003; Document XIII-1990-03.
- [33 ] Fricke W, Doerk O. Simplified approach to fatigue strength assessment of fillet-welded attachment ends. *Int J Fatigue* 2006; 28:141-150.
- [34 ] Lazzarin P., Berto F. (2008). Control volumes and strain energy density under small and large scale yielding due to tensile and torsion loading, *Fatigue and Fracture of Engineering Materials and Structures*, 31, 95-107.
- [35 ] Ellyin F., *Fatigue Damage, Crack Growth and Life Prediction*, Chapman & Hall, London, 1997.